Journal Homepage: http://ijcpe.uobaghdad.edu.iq
Iraqi Journal of Chemical and Petroleum Engineering
Vol. 25 No. 1 (March 2024) 23 – 35
EISSN: 2618-0707, PISSN: 1997-4884

Utilizing Hybrid RO-OARO Systems as New Methods for Desalination Process

Hassanain A. Hassan [a, *], Ahmed Faiq Al-Alawy [a], Muayad Al-shaeli [b]

a Department of Chemical Engineering, College of Engineering, University of Baghdad, Baghdad, Iraq
b Paul Wurth Chair, Faculty of Science, Technology and Medicine, University of Luxembourg, Esch-sur-Alzette, Luxembourg

Abstract

The scarcity of fresh water and its essential role in sustaining life on Earth have motivated researchers to seek new, low-cost, scalable technologies for water desalination. Therefore, the osmotically assisted reverse osmosis (OARO) membrane process presents an innovative approach to achieve moderate water recoveries from high salinity water without undergoing a phase change. This work aims to investigate the performance of hybrid RO-OARO systems with various designs and operational parameters on recovery and R%. The hybrid systems were evaluated for 60 minutes at feed concentrations of 3.98-5.54 g/l, applied pressures ranging from 3 to 7 bars, and different membrane types. The results showed that the flux of the hybrid system increased by increasing the pressure and decreased by increasing the feed concentration. The highest recovery value was obtained for the RO-OARO system at an RO pressure of 7 bar and an OARO unit at 3 bar for a 3.98 g/l feed concentration. In contrast, when the reverse osmosis pressure was fixed at 5 bar, and the pressure of the OARO unit increased by 2 bar, the recovery value exceeded by about 6%. Furthermore, the FilmTech membrane showed the highest recovery at 31.7%, while the highest R% was 94.55% for the AquaTec membrane. The RO-OARO-OARO system contributed to increasing both the recovery and rejection values by 11.4 and 2.1%, respectively, compared with the RO-OARO system. The experiments in this study revealed a slight increase in the feed concentration of the reverse osmosis unit, indicating the efficiency of the hybrid systems compared to traditional RO systems.

Keywords: hybrid; reverse osmosis; osmotically assisted reverse osmosis; desalination.

Received on 05/10/2023, Received in Revised Form on 17/12/2023, Accepted on 17/12/2023, Published on 30/03/2024

https://doi.org/10.31699/IJCPE.2024.1.3

1- Introduction

The scarcity of freshwater is a global issue that worsens as population growth and consumption increase [1–4]. Only 2.5% of the global water supply can be classified as freshwater, while the remaining portion is categorized as saline [5,6]. The need for pure water sources is rising steadily as the economy and population rise, where freshwater scarcity and drinking water safety have become major impediments to long-term socioeconomic growth in areas with limited freshwater resources [7]. Desalination is one of the most promising alternatives for resolving water scarcity [8], in which fresh water is extracted from saline water sources. Desalination has been employed globally to remove salts from seawater (67%), brackish water (19%), river water (8%), and wastewater (6%), respectively [9,10]. Desalination processes are generally classified into two types: the first type is the thermal or phase-change process, and the second type is the membrane process separation [11]. Multi-stage flash distillation (MSF), multi-effect distillation (MED), membrane distillation (MD), and mechanical vapor compression (MVC) are the most common thermal change processes. On the other hand, reverse osmosis (RO), forward osmosis (FO), and electrodialysis (ED) are the most popular membrane separation processes, in which the salt is removed, and drinkable water is produced immediately after using specialized membranes [12].

Reverse osmosis membranes are extensively utilized in various applications, including wastewater purification, drinking water treatment, seawater desalination, food and dairy industries, and medical applications [12–15]. In addition to RO, the forward osmosis membrane technology is also considered one of the most promising technologies for purifying water and wastewater, which has widespread use [4, 17]. Recent advancements in the RO area have resulted in new technologies named according to the research team as follows: reverse osmosis system with recirculation (RRO) [18], osmotically assisted reverse osmosis (OARO) [18–24], draw solution assisted reverse osmosis (DSARO) [25], osmotically enhanced dewatering reverse osmosis (OED-RO) [26, 27], cascading osmotically mediated reverse osmosis (COMRO) [28], split-feed counter-flow (or co-flow) reverse osmosis (split-feed CFRO) [29], osmotically enhanced reverse osmosis (OERO) [30], and osmotically assisted solvent reverse osmosis [31].

The OARO has a 4-port membrane module, so the low-pressure (L.P.) side faces the support layer of the membrane while the high-pressure (H.P.) side faces the

*Corresponding Author: Email: hassanain.abbas@coeng.uobaghdad.edu.iq

active layer of the membrane. In this configuration, the osmotic concentration (i.e., osmotic pressure) on the L.P. side is equal to that of the feed solution on the H.P. side to reduce the osmotic pressure difference (Δπ) across the membrane, as illustrated in Fig. 1 [19, 32]. OARO is a pressure-driven membrane-based system combining RO and FO principles [6, 3]. Since the osmotic pressure difference across the membrane is small or negligible, water can pass through the membrane by applying pressure regardless of the feed concentration, according to Eq. 1 [21].

$$J_w = A[(P_H - P_L) - (\pi_{H,m} - \pi_{L,m})] \quad (1)$$

Where, J_w is the water flux, and P_H and P_L are the applied pressures for both H.P. and L.P. sides, respectively. $\pi_{H,m}$ and $\pi_{L,m}$ are the osmotic pressures of H.P. and L.P. sides at the surface of the membrane.

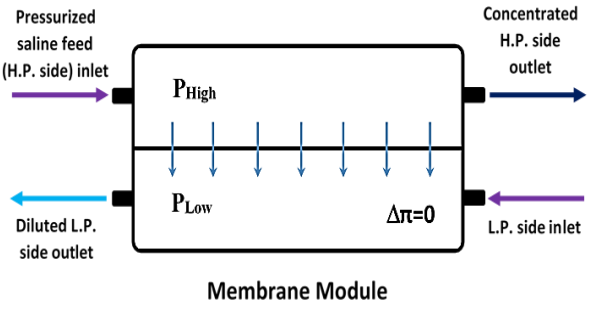

Fig. 1. Schematic of the Membrane Module

As the water permeates from the H.P. side to the L.P. side in this scenario, the concentration on the H.P. side increases, and the concentration on the L.P. side decreases [26, 32]. After one or more than one stages, the diluted stream is pressurized to a moderate pressure difference ΔP and desalinated in a final traditional RO stage, resulting in the production of freshwater [28]. As a result, the OARO process decreases energy costs and prevents membrane damage caused by pressure. In addition, equipment costs can be predicted to be reduced because there is no requirement for high-pressure-resistant material for pipelines and modules [20]. The ability to achieve substantial system recoveries at comparatively lower energy costs and operating pressures makes OARO systems economically viable alternatives to current brine dewatering techniques. Pressure-driven membrane processes are much more energy efficient than their thermal counterparts. H.P. RO and OARO systems can be combined to treat high brine concentrations economically and sustainably. This capability will allow pressure-driven membrane processes, such as H.P. RO and OARO systems, to compete with or entirely replace thermal technologies [23]. The main objective of this work is to design and test a hybrid system combining RO and OARO. The goal is to achieve high recovery (i.e., high flux) and a high rejection percentage (i.e., the lowest permeate concentration). The study will investigate the impact of applied pressure, feed concentration, and membrane type on both recovery and rejection percentage.

2- Experimental Work

Laboratory-grade sodium chloride (NaCl) with a purity of 99.9% (Central Drag House (P) Ltd., India) and distilled water with a purity of 1.7 µS/cm were used to prepare the feed and sweep solutions with varying initial concentrations. The lab scale hybrid RO-OARO system shown in Fig. 2 contains the following parts: the RO module contains the housing of the membrane, where one of its sides contains one port for entering the feeding solution, and the other contains two ports, one for the exit of the concentrated solution and the other for the exit of permeate water. On the other hand, the OARO system requires a 4-port configuration. Therefore, the RO housing element was modified to incorporate two ports on each side, two ports for the inlet streams of the H.P. and L.P. sides, and two ports for their outlet streams**.** Five diaphragm pumps (Model: PROLIFE DP-75, China) were utilized to pump the feed solution through both the OARO module on the H.P. and L.P. sides, as well as the RO module on the feed stream side of the membrane. Polyamide thin-film composite (TFC) membranes of spiral-wound elements were locally assembled of different types and origins, usually used for RO application. Table 1 shows the specifications of the RO spiral-wound elements used in this work.

The water permeation flux ($J_{w,p}$) was determined with a digital mass balance to measure the weight change of the solution according to Eq. 2. The $J_{w,p}$ (l/m^2.h, abbreviated as LMH) is calculated from changing the volume ΔV over test duration Δt [3, 33].

$$J_{w,p} = \frac{\Delta V}{A_m \Delta t} \quad (2)$$

Where: ΔV (L) represents the volume change of solution for the duration of the test Δt (hr), and A_m (m^2) is the effective area of the membrane. The recovery measures how much of the feed is recovered as permeate; it is reported as a percentage. The recovery was determined by using Eq. 3 [34, 35].

$$Recovery\ \% = \left(\frac{Q_P}{Q_F}\right) \times 100\% \quad (3)$$

Where: Q_P is the volumetric flow rate of water transferred to the permeate side (representing the accumulated volume of permeated water per the total time of the experiment), and Q_F is the volumetric flow rate of the feed solution. The salt rejection was obtained using Eq. 4 [36].

$$R\ \% = \left(1 - \frac{C_p}{C_f}\right) \times\ 100\% \quad (4)$$

Where: C_p is the permeate concentration of salts on the permeate side, and C_f is the concentration of salts on the feed solution side.

Fig. 2. The Lab Scale of the Hybrid RO-OARO System

Table 1. Specifications of RO Spiral-Wound Elements

Membrane		Hi-Tech RO Element	FilmTec™ Element	AquaTec RO Element
Model		**RE-1812-75 (Thailand)**	**TW30-1812-100HR (USA)**	**Model:100 GPD (China)**
Performance	Max. Salt Rejection (%)	97-98	98	98-99
	Permeate Flow (l/min)	0.189	0.315	0.17
	Diameter (cm)	4.57	4.45	4.50
	Length (cm)	30.48	29.8	29
Testing Condition	Testing Pressure (bar)	4.83	3.4	4-5
	Testing Temperature (°C)	25	25	25
	pH Value of Testing Solution	6.0 -7.5	2-11	5-8
	Concentration of testing Solution (NaCl) (ppm)	1500	250	300-3000
	Recovery Rate (Single Element) (%)	20	15	20

2.1. Description of Hybrid RO-OARO System

The combination of both RO and OARO units was used in this design. The experimental setup for the hybrid RO-OARO system is shown in Fig. 3. The vessels V.01 and V.04 were filled with a certain amount of solution as a start-feeding solution for both RO and OARO, respectively. The inlet streams of the OARO module for both the H.P. and L.P. sides were supplied from V.04 to ensure that the osmotic pressure difference ($\Delta\pi$) across the membrane becomes 0 at any time during the experiment. As shown in Fig. 3, the permeate stream leaving the RO module was collected in vessel V.02. Additionally, the concentrated stream was poured into V.04. The diluted stream in the existing L.P. side was poured into V.01, which contributed to reducing or stabilizing the concentration of the vessel. Furthermore, the concentrated stream in the existing H.P. side was collected in vessel V.03.

In this system, feed solution concentrations of about 4 and 5.5 g/l were used. Vessels V.01 and V.04 were filled with NaCl solution. The applied pressure in the hybrid RO-OARO system used was 5 and 7 bar for the RO unit, while it was 3 and 5 bar for the H.P. side of the RO and 3 bar and 5 bar for the H.P. side of the OARO unit, corresponding to the used concentrations. The flow rate of all inlet streams was set at 0.25 l/min. The differences in weight vessels and the solution concentrations were recorded every 15 min. NaCl salt scales were removed from the apparatus by flushing it with distilled water at the end of the experiment. Table 2 represents the range of the operating conditions examined in the hybrid RO-OARO system.

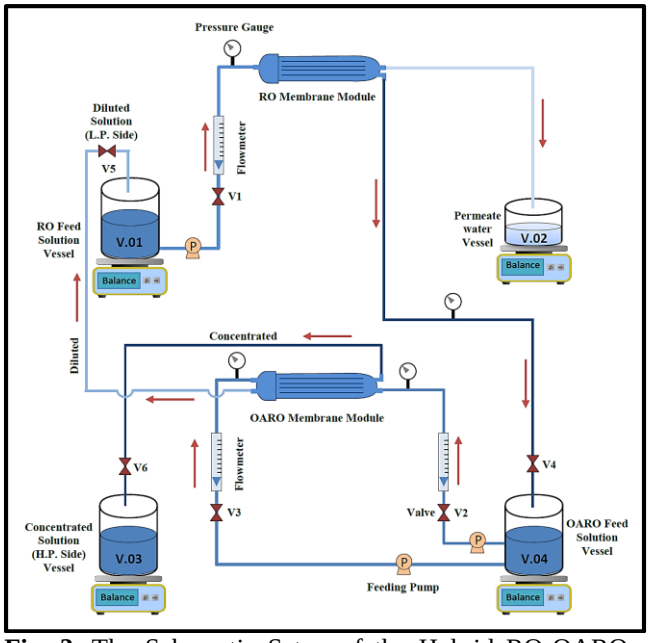

Fig. 3. The Schematic Setup of the Hybrid RO-OARO System

Table 2. Operating Conditions of the Hybrid RO-OARO System

Operating Conditions	
Applied pressure of the RO unit	5 and 7 bar
Applied pressure of H.P. side of the OARO unit	3 and 5 bar
Feed solution concentration	≈ 4 and 5.5 g/l
Inlet flow rates of RO, L.P. and H.P. sides	0.25 l/min

2.2. Description of Hybrid RO-OARO-OARO System

The quality of the permeate water flux produced by the RO unit could be improved by maintaining the concentration of the RO feed solution at or below its starting concentration. To achieve this, a hybrid RO-OARO-OARO system was employed, involving the collaboration of two OARO units and one RO unit. Additionally, this design aimed to enhance the overall recovery value.

The vessels V.01, V.03, and V.04 were initially filled with a solution at a concentration of 4.02 g/l, serving as the starting feed solution for both the Reverse Osmosis (RO) and Osmotically Assisted Reverse Osmosis (OARO) units. For OARO1 and OARO2, the inlet streams on both the H.P. and L.P. sides were sourced from vessels V.03 and V.04, respectively. The schematic diagram of the hybrid RO-OARO-OARO system is depicted in Fig. 4. The permeate stream exiting the RO module was collected in V.02, while the concentrated stream was directed into V.03. While, the concentrated stream from the H.P. side of OARO1 was directed into V.04, and the stream leaving the H.P. side of OARO2 was collected in vessel V.05. The diluted stream from the L.P. sides of both OARO1 and OARO2 was directed into V.01, contributing to the maintenance of a constant level and concentration in vessel V.01 (i.e., the feed solution of the RO unit) throughout the experiment.

In the hybrid RO-OARO-OARO system, the applied pressures were set at 5 bar for the RO unit and 3 bar for both the H.P. sides of OARO1 and OARO2 units. The inlet stream flow rate was fixed at 0.25 l/min. Weight variations in the vessels and solution concentrations were monitored at 15 min intervals. Therefore, the system underwent cleaning with distilled water (DI). Table 3 summarize the operating conditions for the hybrid RO-OARO-OARO System.

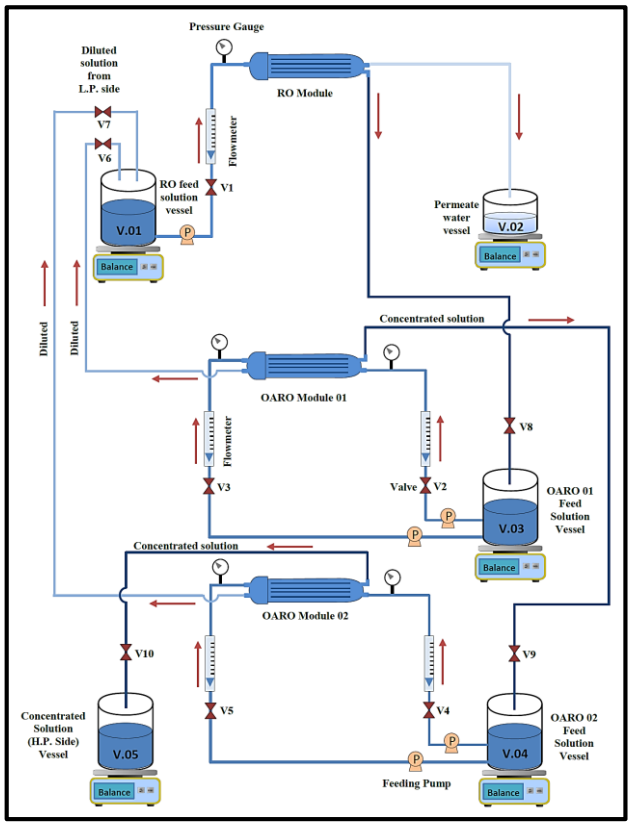

Fig. 4. The Schematic Setup of the Hybrid RO-OARO-OARO System

Table 3. Operating Conditions for the Hybrid RO-OARO-OARO System

Operating Conditions	
Applied pressure of RO unit	5 bar
Applied pressure for H.P. sides of OARO1 and OARO2 units	3 bar
Feed solution concentration	4.02 g/l
Inlet flow rates of RO, L.P. and H.P. sides	0.25 l/min

3- Results and Discussions

3.1. Hybrid RO-OARO System

This system combined the work of both RO and OARO processes. This design aimed to keep the solution in the feeding vessel of the RO stage more diluted, stabilized, or as less concentrated as possible throughout the experiment. This was achieved by supplying the RO feeding vessel with the diluted solution from the outlet stream of the low-pressure (L.P.) side of the OARO unit.

- Effect of Reverse Osmosis Module Pressure

The effect of changing the applied pressure of RO stage on permeate water flux ($J_{w,p}$), the concentration of

permeate water (C_p), the RO feed solution concentration (C_f), and the concentration of the feed solution vessel of OARO (C_{OARO}) were investigated and the results are presented in Fig. 5. For the feed solution of ≈4 g/l and the applied pressure on the H.P. side of the OARO module fixed at 3 bar, the permeate water flux increased by 111.8% after 60 min as the applied pressure of RO stage increased from 5-7 bar (Fig. 5a). However, it is noteworthy that the flux slightly decreased with time, approximately 7.5% for RO at 5 bar and 12.5% for RO at 7 bar. This decrease is attributed to the slight increment in the concentration of RO feed solution (C_f) with time. C_f changes slightly, either increasing or decreasing due to the concentration of the dilute solution from the OARO unit (C_{OARO}), as shown in Fig. 5b. Additionally, the decrease in flux value may result from the accumulation of salt on the surface of the membrane and the appearance of the effect of external concentration polarization (ECP). It is clear from Fig. 5b, that the concentration of the RO feed solution at a pressure of 7 bar was higher than that at a pressure of 5 bar because the amount of water permeating through the membrane was higher at 7 bar, thus making the solution was more concentrated.

Fig. 5c depicts the concentration response of permeate water (C_p) over time. When the experiment started, the C_p value decreased during the initial 15 min, influenced by the concentration of the RO feed solution (C_f). Subsequently, the C_p value tends to stabilize during the final 30 min of the experiment. This stability in C_p is attributed to a slight increase in C_f. It is anticipated that with the experiment's prolonged duration, the C_p value may either increase or remain constant due to variations in C_f. Fig. 5d illustrates the fluctuation in the concentration of the feed solution vessel of OARO over time at different applied pressures of RO. The rejected stream from the RO unit representing the concentrated stream is directed into the feed solution vessel of OARO. In the case of running RO at 7 bar, this stream is more concentrated compared to that at 5 bar, resulting in a higher concentration in the feed solution vessel of OARO.

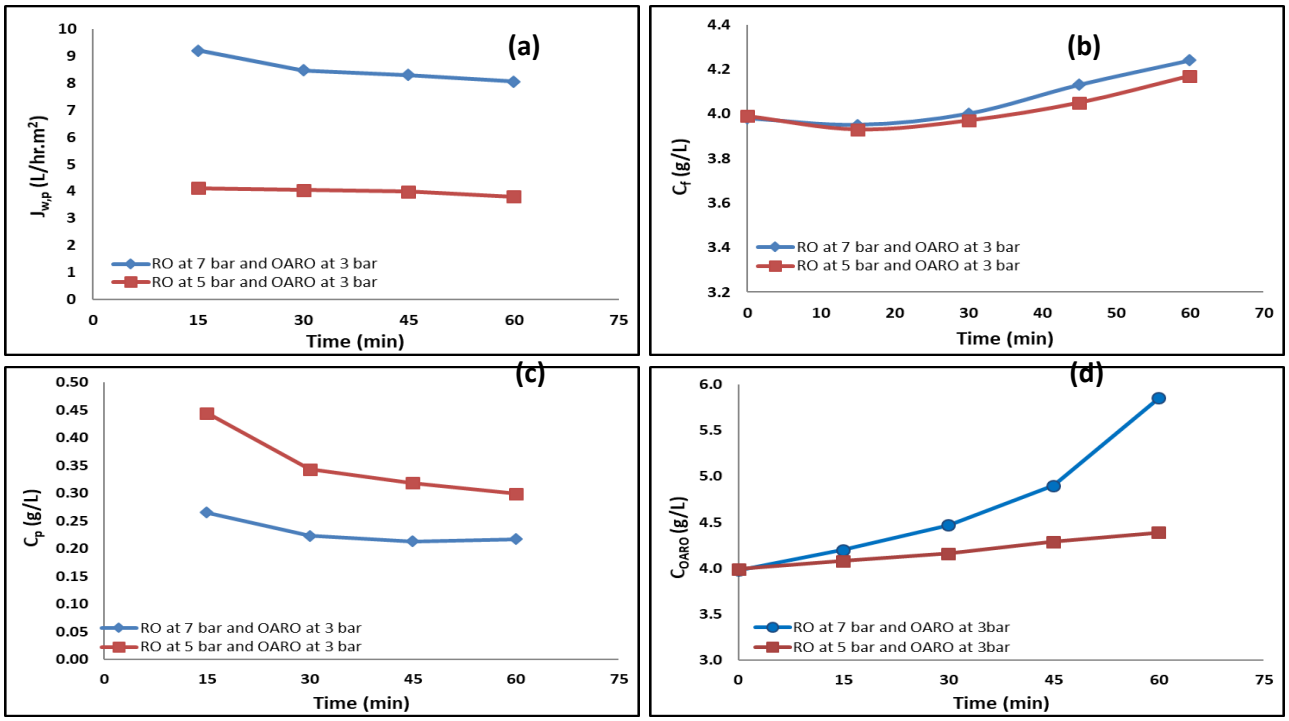

Fig. 5. (a) Flux of Permeate Water ($J_{w,p}$), (b) Concentration of RO Feed Solution (C_f), (c) Concentration of Permeate Water (C_p), and (d) Concentration of OARO Feed Solution (C_{OARO}) as a Function of Time for the Feed Concentration of ≈ 4 g/l and Different RO Applied Pressures

- Effect of Feed Concentration

In this part, the applied pressure for both RO and OARO units was held constant. The concentration of the feed solution was changed from 3.98 to 5.54 g/l, to investigate the effect of changing the concentration of the feed solution on the $J_{w,p}$, C_p, C_f, and the C_{OARO}. As shown in Fig.6, increasing the feed solution concentration from 3.98 to 5.54 g/l decreased the average flux value by approximately 55% (Fig. 6a). The elevation in the concentration of the RO unit's feed solution resulted in an increased osmotic pressure of the feed (π_f). Consequently, the driving force, represented by ΔP - Δπ, decreased, leading to a reduction in the permeable flux through the membrane as the feed concentration increased.

Furthermore, the influence of changing the feed concentration on the concentration of permeate water is shown in Fig. 6b. It is observed that the C_p value increased with increasing the concentration of the feed solution. When the feed solution concentration increased from 3.98 to 5.54 g/l, the average value of the C_p increased by about 26%. This increase in C_p was attributed the higher concentration of the RO feed solution C_f, resulting in an increased salt flux.

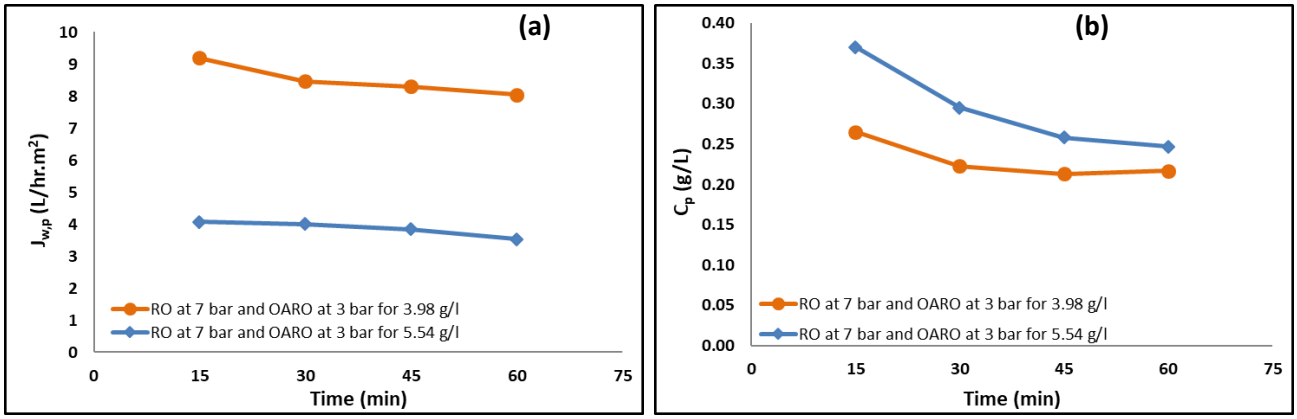

Fig. 6. (a) Flux of Permeate Water ($J_{w,p}$) and (b) Concentration of Permeate Water (C_p) as a Function of Time for Different Feed Concentrations

- Effect of OARO Module Pressure

In the next stage, the feed solution concentration was fixed at ≈4 g/l, the applied pressure was fixed at 5 bar for the RO module and varied from 3 to 5 bar on the H.P. side of the OARO module. The effect of changing the applied pressure of the OARO stage was examined, as shown in Fig. 7. When the applied pressure changed from 3 to 5 bar, the water flow increased from the H.P. side to the L.P. side, leading to a decrease the concentration of the OARO unit (C_{OARO}) feed solution, as shown in Fig. 7a. As a result, the stream that pours in the vessel of RO became more diluted than that when the pressure of OARO at 3 bar. Consequently, the stream pouring into the vessel of RO became more diluted compared to the OARO pressure running at 3 bar. This improvement in the quality of the RO feed solution resulted in reduced values of C_f, as shown in Fig. 7b. This positive effect on the permeate water flux was evident when the pressure changed from 3 to 5 bar and obtaining a reduced value of C_p as depicted in Fig. 7c and d, respectively.

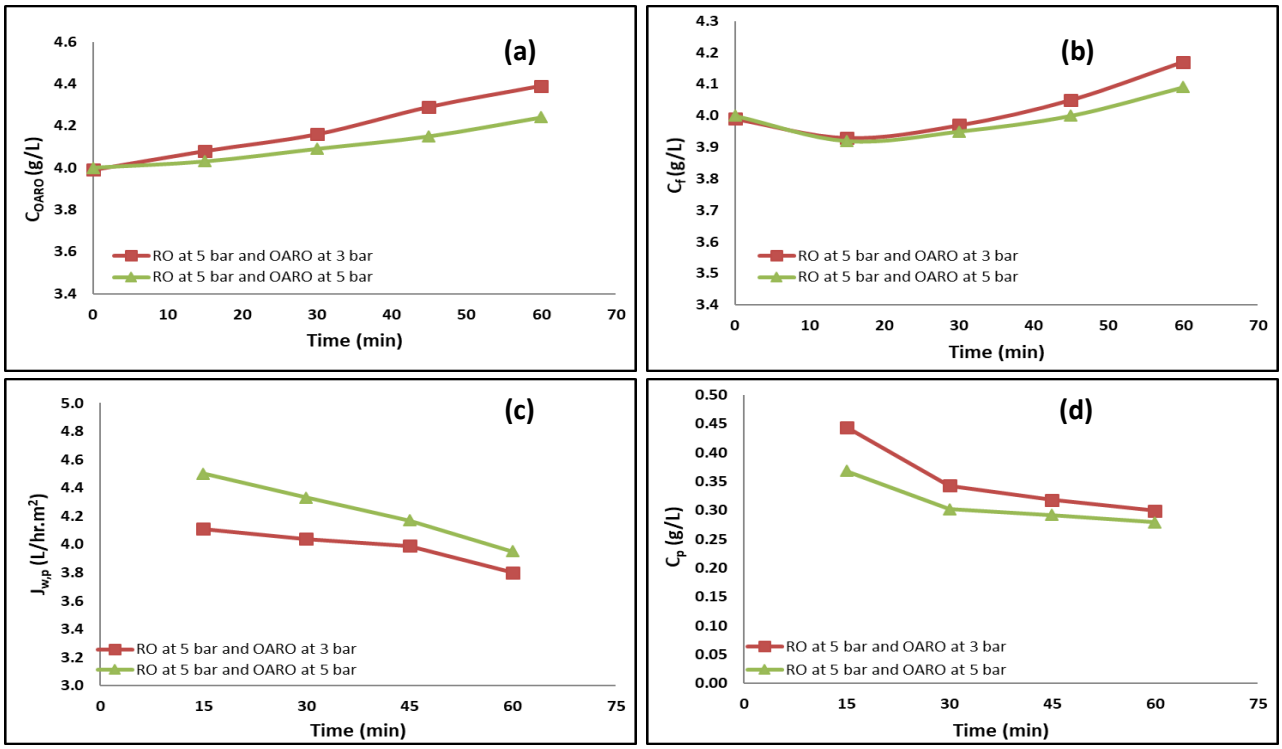

Fig. 7. (a) Concentration of OARO Feed Solution (C_{OARO}), (b) Concentration of RO Feed Solution (C_f), (c) Flux of Permeate Water ($J_{w,p}$), and (d) Concentration of Permeate Water (C_p) as a Function of Time for Different OARO Applied Pressures

- Membrane Type Effect

A comparative analysis was conducted for different types of commercial spiral wound membranes (Model: AquaTec, Hi-Tech, and FilmTech) to investigate their performance. Experiments were carried out for the hybrid RO-OARO under specific conditions of feed

concentration and applied pressures (≈3.99 g/l, RO at 7 bar and H.P. side of OARO at 3 bar). Initially, RO tests was performed to determine the water permeability coefficient values of the different membranes. Fig. 8 illustrates the relationship between the water flux of RO membrane and the hydraulic applied pressure. As shown in Fig. 8, the water flux increased steadily as the applied pressure was raised from 1 to 5 bar, demonstrating that the water flux through the membrane was linearly proportional to the hydraulic pressure across the membrane according to Eq. 1. The water permeability coefficient (A) represents the slope of the best-fitting line obtained for each membrane, where it was 11.47 for FilmTech, 9.16 for Hi-Tech, and 8.23 LMH/bar for AquaTec.

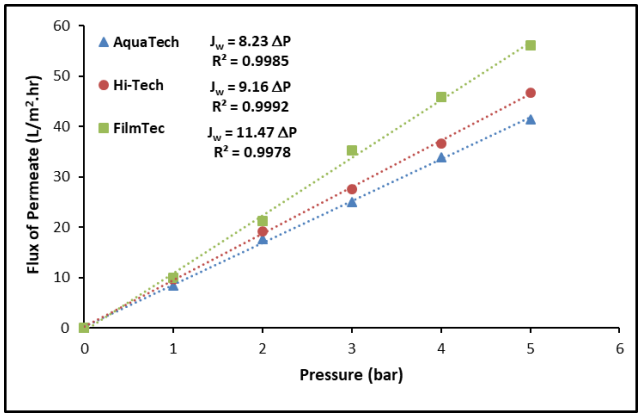

Fig. 8. Permeability for the Different Types of Membranes

RO experiments were conducted at 6 bar and 5 g/l NaCl feed solution to determine each membrane's salt permeability coefficient (B). The results are shown in Table 4, where Eq. 5 was used to calculate B [37].

$$B = \frac{A(\Delta P - \Delta\pi)(1 - R)}{R} \quad (5)$$

Where A is the water permeability, R is the salt rejection, ΔP is the applied pressure difference, and $\Delta\pi$ is the osmotic pressure difference.

Table 4. Salt Permeability Coefficient (B) RO Test Results at 6 bar and 5 g/l NaCl Feed Solution

Membrane Type	Permeate Concentration (mg/l)	Salt Permeability Coefficient (B) (m/s)
FilmTech	0.564	8.67×10^{-7}
Hi-Tech	0.58	7.19×10^{-7}
AquaTec	0.229	2.03×10^{-7}

The three membranes were compare based on the value of water permeate flux and Recovery%, as depicted in Fig. 9. It was observed that the FilmTech membrane exhibited the highest flux values compared to the other membranes, followed by the Hi-Tech and then the AquaTec membrane (Fig. 9a). These flux values were reflected in the recovery values obtained, with the FilmTech membrane showing about a 30% excess in recovery compared to AquaTec, as illustrated in Fig. 9b. Otherwise, when comparing the removal performance of the membranes, the AquaTec membrane exhibited lower C_p values (i.e., higher R %) than the other membranes, as seen in Fig. 10, where the R % followed the order AquaTec > Hi-Tech > FilmTec. The differences in fluxes and C_p values between the membranes can be attributed to variations in the water and solute permeability coefficients, as illustrated in Fig. 8 and Table 4. In other words, B values of the AquaTec membrane was 76.7% lower than FilmTech and 71.81% lower than Hi-Tech membranes, resulting in a higher R % in the AquaTec membrane. These results align with those obtained by Salih et al. (2023).

The disparity between the flux values for the membranes led to a difference in their C_f values, where the FilmTech membrane showed higher C_f values than the other membranes, as shown in Fig. 11a. The excess percentage for the feed solution concentration of the RO unit after 60 min was 10.8, 7.8, and 6.5 for the FilmTech, Hi-Tec, and AquaTec membranes, respectively (Fig. 11b). From these results, it can be concluded that if the goal is the quantity and not the quality of desalinated water, such as in the case of water used for irrigation purposes, the FilmTech membrane is preferred. In contrast, if the goal is quality regardless of the resulting quantity of water, as in the case of water used for drinking or heat exchangers, then AquaTec membrane is recommended.

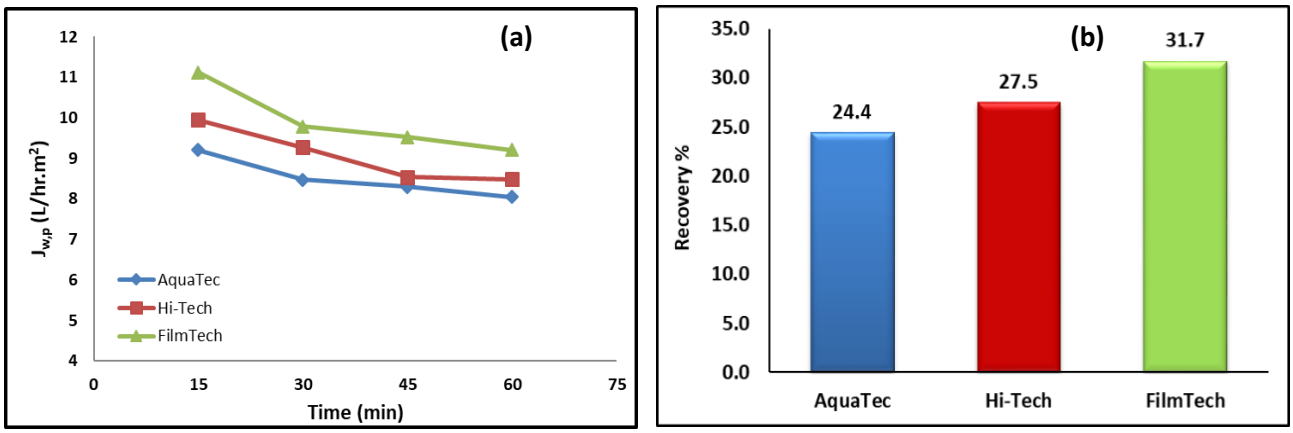

Fig. 9. (a) Flux of Permeate Water ($J_{w,p}$), and (b) Recovery % as a Function of Time for Different Membranes

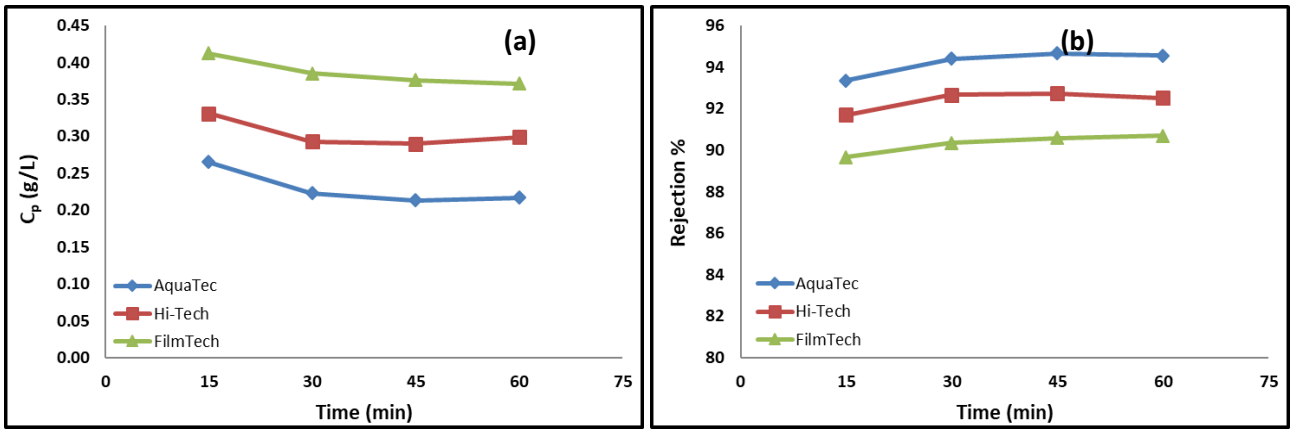

Fig. 10. (a) Concentration of Permeate Water (C_p), and (b) R% as a Function of Time for Different Membranes

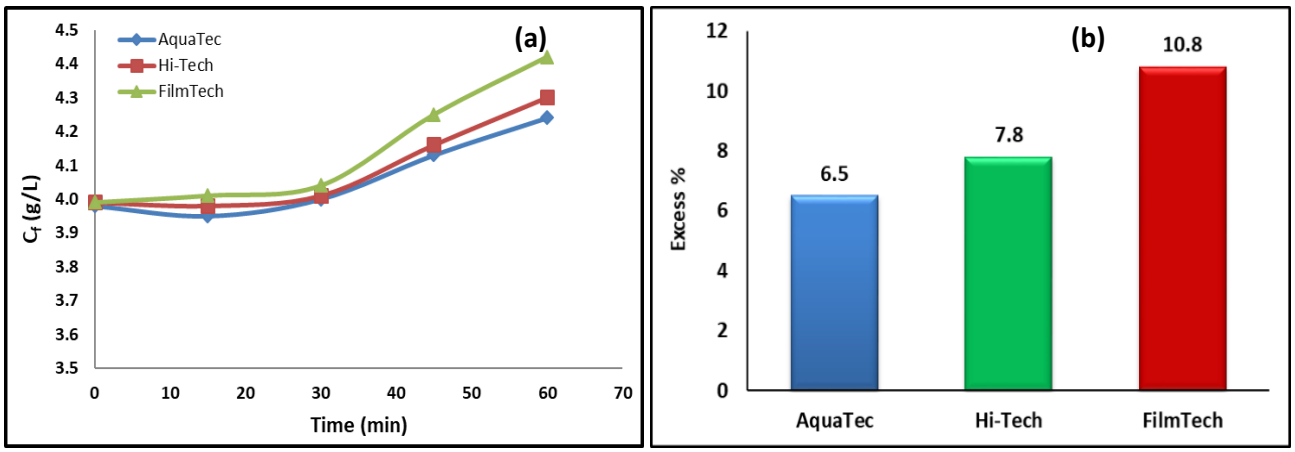

Fig. 11. (a) The concentration of RO Feed Solution (C_f), as a Function of Time, and (b) RO Feed Concentration Excess % after 60 min for Different Membranes

- Assessment of Hybrid RO-OARO System

A comparison was made for the hybrid RO-OARO at different concentrations and different applied pressures, as shown in Fig. 12 - Fig. 14. It can be seen from Fig. 12 that the highest recovery% value for was 24.4% for RO at 7 bar and OARO at 3 bar for 3.98 g/l feed concentration, and the other recovery values ranged between 11.1 to 12.8% for the other applied pressures and feed concentrations. Additionally, the most favorable R% response was observed for RO at 7 bar and OARO at 5 bar with a feed concentration of 5.53 g/l, achieving a maximum value about 96%, as depicted in Fig. 13. When comparing the initial and final concentrations of the feed solution for the RO unit, it is evident that the optimal dilution occurred for the feed solution of the RO unit. This can be inferred from the final C_f value, which was 4.09 g/l for RO at 5 bar and OARO at 5 bar with a feed concentration of 4 g/l, and 5.58 g/l for RO at 7 bar and OARO at 5 bar with a feed concentration of 5.53 g/l, as shown in Fig. 14.

3.2 Hybrid RO-OARO-OARO System

Maintaining the feed solution concentration in the RO unit at or below its initial concentration is crucial for enhancing the quality of the permeate produced by the RO unit. To achieve this objective, a hybrid RO-OARO-OARO system incorporating one stage of RO and two OARO modules operating is recommended. The design also aimed to maximize the achieved Recovery%. The experiment was conducted at a feed solution concentration of 4.02 g/l, and the applied pressure on the H.P. side of the OARO1 and OARO2 modules was set at 3 bars, while the applied pressure on the RO module was set at 7 bars. The results were compared with those of the hybrid RO-OARO system with a feed concentration of 3.99 g/l, and the applied pressures on the RO and the H.P. side of the OARO modules were 5 and 3 bars, respectively.

Fig. 4 shows that the dilute streams from the OARO1 and OARO2 units contributed to the dilution and stabilization of the feed concentration in the RO unit. The C_f value increased by only 2% during the experiment, as depicted in Fig. 15. Additionally, the C_f values for the two-stage OARO system were lower than those of the one-stage system. This decrease effectively increased the flux, recovery%, and RR values (Fig. 16 and Fig. 17). The Recovery% value increased from 11.4% to 12.7%, and the R% increased from 92.51% to 94.45%. The improvement in the quality of the feed solution of the RO unit also contributed to enhancing the permeate water

quality, as indicated by the C_p values in Fig. 18. The excess percentage of flux and rejection over time is presented in Fig. 19, where the excess percentage values were initially high and gradually decreased over the experiment.

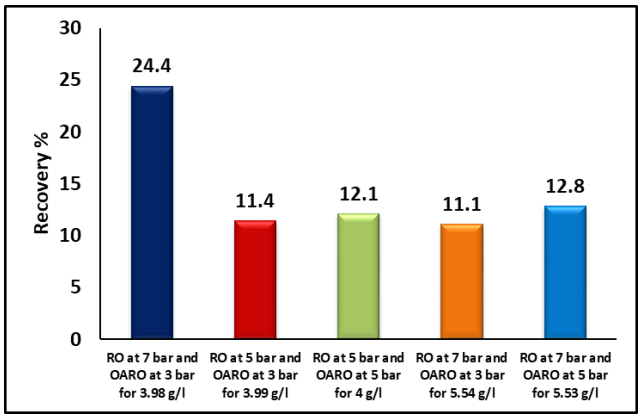

Fig. 12. Comparison of Recovery % after 60 min for Different Feed Concentrations and Different Applied Pressures

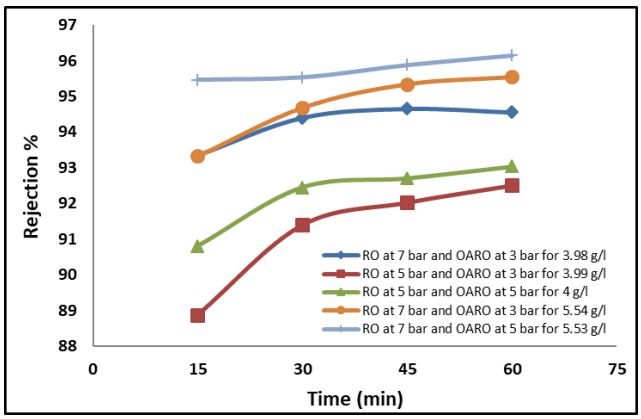

Fig. 13. Comparison of R % for Different Feed Concentrations and Different Applied Pressures

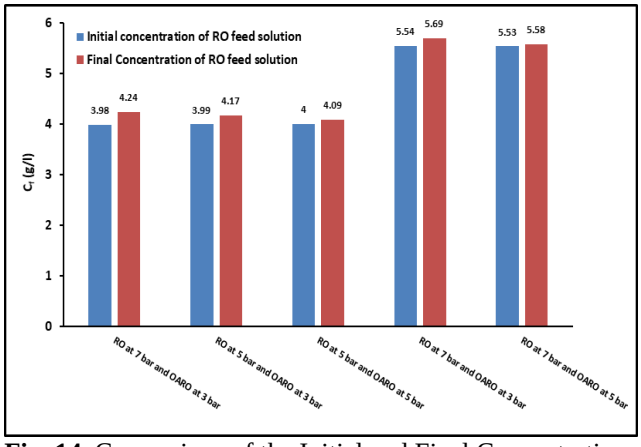

Fig. 14. Comparison of the Initial and Final Concentration of RO Feed Solution for Different Conditions of Hybrid RO-OARO System

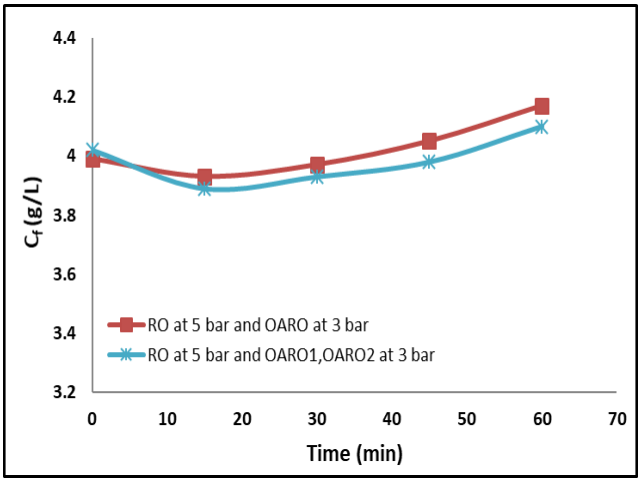

Fig. 15. Comparison of C_f as a Function of Time for Systems (I) and (II)

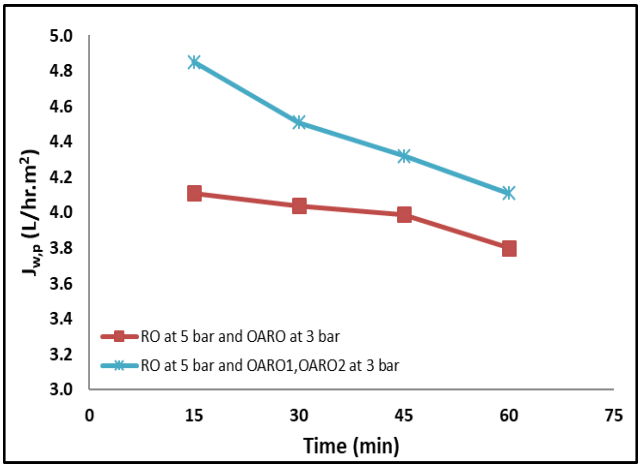

Fig. 16. Comparison of Water Permeate Flux ($J_{w,p}$) as a Function of Time for Systems (I) and (II)

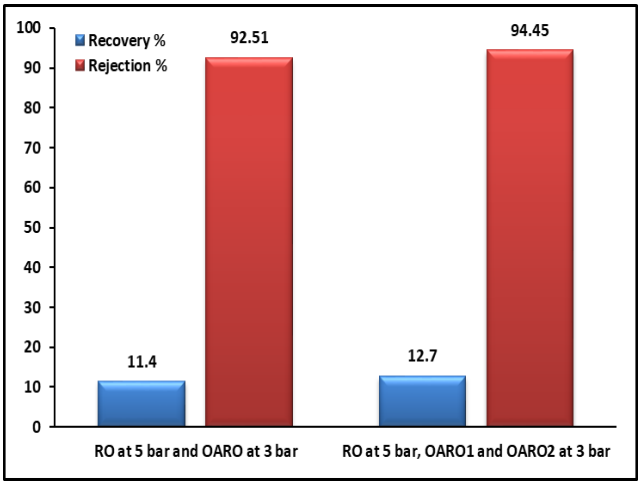

Fig. 17. Comparison of Recovery % and R% after 60 min for Systems (I) and (II)

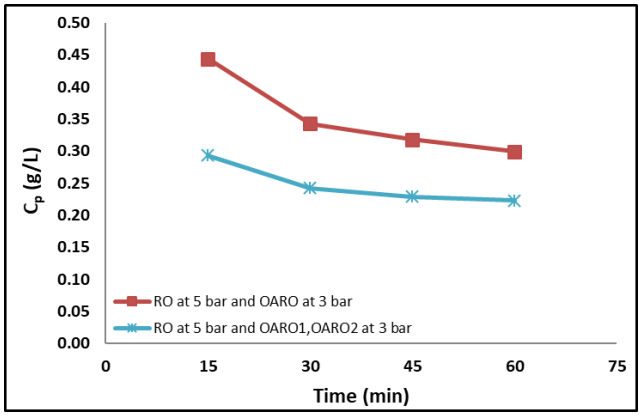

Fig. 18. Comparison of C_p as a Function of Time for Systems (I) and (II)

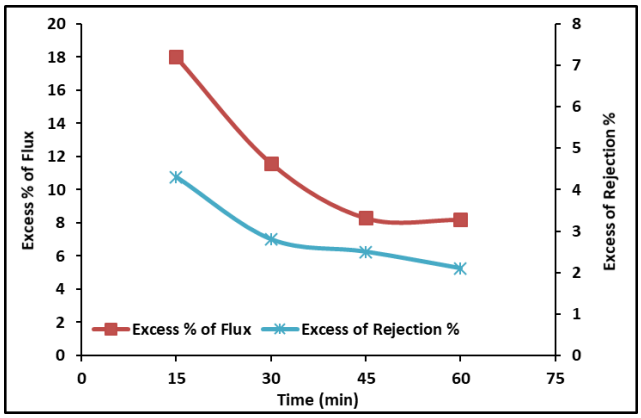

Fig. 19. Comparison of Excess % of Flux and R% as a Function of Time for Systems (I) and (II)

4- Conclusions

The present study demonstrates the efficiency of the hybrid system, which combines RO and OARO units for desalination, yielding favorable recovery and rejection percentage values. The highest flux achieved from the hybrid RO-OARO system was 8.05 L/hr.m², with an R% of 94.55% at a feed concentration of 3.98 g/l, RO pressure of 7 bars, and OARO pressure of 3 bars over 60 min. Additionally, the recovery increased from 11.1% to 12.8% as the applied OARO pressure rose from 3 to 5 bars at approximately 5.53 g/l feed concentration. The R% of the different membranes in this study followed the order: AquaTec (94.55%) > Hi-Tech (92.51%) > FilmTech (90.7%). Conversely, the FilmTech membrane exhibited the highest recovery value compared to the other membranes. The introduction of an additional OARO unit to the RO-OARO system contributed to an 11.4% increase in recovery.

References

[1] A. F. Al-Alawy and R. M. Al-Alawy, "Thermal Osmosis of Mixtures of Water and Organic Compounds through Different Membranes," *Iraqi Journal of Chemical and Petroleum Engineering*, vol. 17, no. 2 SE-Articles, pp. 53–68, Jun. 2016, https://doi.org/10.31699/IJCPE.2016.2.7

[2] A. F. Al-Alawy and M. H. Salih, "Experimental Study and Mathematical Modelling of Zinc Removal by Reverse Osmosis Membranes," *Iraqi Journal of Chemical and Petroleum Engineering*, vol. 17, no. 3, pp. 57–73, 2016, https://doi.org/10.31699/IJCPE.2016.3.5

[3] F. A. Yaseen, A. F. Al-Alalawy, and A. Sharif, "Renewable energy by closed-loop pressure retarded osmosis using hollow fiber module," *AIP Conference Proceedings*, vol. 2213, no. 1, p. 20201, Mar. 2020, https://doi.org/10.1063/5.0000156

[4] R. M. Kadhim, E. E. Al-Abodi, and A. F. Al-Alawy, "Citrate-coated magnetite nanoparticles as osmotic agent in a forward osmosis process," *Desalination and Water Treatment*, vol. 115, no. January, pp. 45–52, 2018, https://doi.org/10.5004/dwt.2018.22456

[5] A. Alkaisi, R. Mossad, and A. Sharifian-Barforoush, "A Review of the Water Desalination Systems Integrated with Renewable Energy," in *Energy Procedia*, vol. 110, pp. 268–274, 2017, https://doi.org/10.1016/j.egypro.2017.03.138

[6] B. Al-Najar, C. D. Peters, H. Albuflasa, and N. P. Hankins, "Pressure and osmotically driven membrane processes: A review of the benefits and production of nano-enhanced membranes for desalination," *Desalination*, vol. 479. Elsevier B.V., Apr. 01, 2020, https://doi.org/10.1016/j.desal.2020.114323

[7] J. R. Du, X. Zhang, X. Feng, Y. Wu, F. Cheng, and M. E. A. Ali, "Desalination of high salinity brackish water by an NF-RO hybrid system," *Desalination*, vol. 491, p. 114445, Oct. 2020, https://doi.org/10.1016/J.DESAL.2020.114445

[8] M. H. Salih and A. F. Al-Alawy, "Crystallization Process as a Final Part of Zero Liquid Discharge System for Treatment of East Baghdad Oilfield Produced Water," *Iraqi Journal of Chemical and Petroleum Engineering*, vol. 23, no. 1 SE-Articles, pp. 15–22, Mar. 2022, https://doi.org/10.31699/IJCPE.2022.1.3

[9] M. C. Garg, "Renewable energy-powered membrane technology: Cost analysis and energy consumption," in *Current Trends and Future Developments on (Bio-) Membranes: Renewable Energy Integrated with Membrane Operations*, Elsevier, 2019, pp. 85–110, https://doi.org/10.1016/B978-0-12-813545-7.00004-0

[10] A. Alkhudhiri, N. Darwish, and N. Hilal, "Membrane distillation: A comprehensive review," *Desalination*, vol. 287. pp. 2–18, 2012, https://doi.org/10.1016/j.desal.2011.08.027

[11] S. Liyanaarachchi, L. Shu, S. Muthukumaran, V. Jegatheesan, and K. Baskaran, "Problems in seawater industrial desalination processes and potential sustainable solutions: A review," *Reviews in Environmental Science and Bio/Technology*, vol. 13, no. 2, pp. 203–214, Nov. 2014, https://doi.org/10.1007/s11157-013-9326-y

[12] T. V. Bartholomew, L. Mey, J. T. Arena, N. S. Siefert, and M. S. Mauter, "Osmotically assisted reverse osmosis for high salinity brine treatment," *Desalination*, vol. 421, pp. 3–11, Nov. 2017, https://doi.org/10.1016/j.desal.2017.04.012

[13] M. H. Salih, A. M. Al-Yaqoobi, H. A. Hassan, and A. F. Al-Alawy, "Assessment of the Pressure Driven Membrane for the Potential Removal of Aniline from Wastewater," *Journal of Ecological Engineering*, vol. 24, no. 8, pp. 118–127, 2023, https://doi.org/10.12911/22998993/166283

[14] R. H. Salman, H. A. Hassan, K. M. Abed, A. F. Al-Alawy, D. A. Tuama, K. M. Hussein, H. A. Jabir, "Removal of chromium ions from a real wastewater of leather industry using electrocoagulation and reverse osmosis processes," in *AIP Conference Proceedings*, Mar. 2020, vol. 2213, no. 1, https://doi.org/10.1063/5.0000201

[15] H. A. Aljendeel, "Removal of Heavy Metals Using Reverse Osmosis," *Journal of Engineering*, vol. 17, no. 3, 2011. https://doi.org/10.31026/j.eng.2011.03.23

[16] W. Bai, L. Samineni, P. Chirontoni, I. Krupa, P. Kasak, A. Popelka, N. B. Saleh, and M. Kumar, "Quantifying and reducing concentration polarization in reverse osmosis systems," *Desalination*, vol. 554. Elsevier, p. 116480, May 15, 2023, https://doi.org/10.1016/j.desal.2023.116480

[17] D. Şahin, "Forward Osmosis Membrane Technology in Wastewater Treatment," in *Osmotically Driven Membrane Processes*, IntechOpen, 2021, https://doi.org/10.5772/intechopen.97483

[18] J. M. Gozálvez, J. Lora, J. A. Mendoza, and M. Sancho, "Modelling of a low-pressure reverse osmosis system with concentrate recirculation to obtain high recovery levels," *Desalination*, vol. 144, no. 1–3, pp. 341–345, Sep. 2002, https://doi.org/10.1016/S0011-9164(02)00341-7

[19] H. A. Hassan and A. F. Al-Alawy, "Osmotically assisted reverse osmosis (OARO) for desalination of brackish water," *AIP Conference Proceedings*, vol. 2806, no. 1, p. 030017, Sep. 2023, https://doi.org/10.1063/5.0163014

[20] N. Togo, K. Nakagawa, T. Shintani, T. Yoshioka, T. Takahashi, E. Kamio, and H. Matsuyama, "Osmotically Assisted Reverse Osmosis Utilizing Hollow Fiber Membrane Module for Concentration Process," *Industrial and Engineering Chemistry Research*, vol. 58, no. 16, pp. 6721–6729, Apr. 2019, https://doi.org/10.1021/ACS.IECR.9B00630

[21] K. Nakagawa, N. Togo, R. Takagi, T. Shintani, T. Yoshioka, E. Kamio, and H. Matsuyama "Multistage osmotically assisted reverse osmosis process for concentrating solutions using hollow fiber membrane modules," *Chemical Engineering Research and Design*, vol. 162, pp. 117–124, 2020, https://doi.org/10.1016/j.cherd.2020.07.029

[22] T. V. Bartholomew, N. S. Siefert, and M. S. Mauter, "Cost Optimization of Osmotically Assisted Reverse Osmosis," *Environmental Science and Technology*, vol. 52, no. 20, pp. 11813–11821, Oct. 2018, https://doi.org/10.1021/ACS.EST.8B02771

[23] C. D. Peters and N. P. Hankins, "Osmotically assisted reverse osmosis (OARO): Five approaches to dewatering saline brines using pressure-driven membrane processes," *Desalination*, vol. 458, pp. 1–13, May 2019, https://doi.org/10.1016/J.DESAL.2019.01.025

[24] C. D. Peters, D. Li, Z. Mo, N. P. Hankins, and Q. She, "Exploring the Limitations of Osmotically Assisted Reverse Osmosis: Membrane Fouling and the Limiting Flux," *Environmental Science and Technology*, 2022, https://doi.org/10.1021/acs.est.2c00839

[25] K. Park, D. Y. Kim, and D. R. Yang, "Cost-based feasibility study and sensitivity analysis of a new draw solution assisted reverse osmosis (DSARO) process for seawater desalination," *Desalination*, vol. 422. pp. 182–193, 2017, https://doi.org/10.1016/j.desal.2017.08.026

[26] J. Kim, D. I. Kim, and S. Hong, "Analysis of an osmotically-enhanced dewatering process for the treatment of highly saline (waste)waters," *Journal of Membrane Science*, vol. 548, pp. 685–693, Feb. 2018, https://doi.org/10.1016/j.memsci.2017.10.048

[27] J. Kim, J. Kim, J. Kim, and S. Hong, "Osmotically enhanced dewatering-reverse osmosis (OED-RO) hybrid system: Implications for shale gas produced water treatment," *Journal of Membrane Science*, vol. 554. pp. 282–290, 2018, https://doi.org/10.1016/j.memsci.2018.03.015

[28] X. Chen and N. Y. Yip, "Unlocking High-Salinity Desalination with Cascading Osmotically Mediated Reverse Osmosis: Energy and Operating Pressure Analysis," *Environmental Science and Technology*, vol. 52, no. 4, pp. 2242–2250, 2018, https://doi.org/10.1021/acs.est.7b05774

[29] A. T. Bouma and J. H. Lienhard, "Split-feed counterflow reverse osmosis for brine concentration," *Desalination*, vol. 445, no. July, pp. 280–291, 2018, https://doi.org/10.1016/j.desal.2018.07.011

[30] X. Li, Y. Mei, J. Zhang, Y. Yang, L. E. Peng, W. Qing, D. He, A. G. Fane, and C. Y. Tang, "Osmotically enhanced reverse osmosis using hollow fiber membranes," *Journal of Membrane Science*, vol. 638, no. May, 2021, https://doi.org/10.1016/j.memsci.2021.119703

[31] Y. H. Chiao, Z. Mai, W. S. Hung, and H. Matsuyama, "Osmotically assisted solvent reverse osmosis membrane for dewatering of aqueous ethanol solution," *Journal of Membrane Science*, vol. 672, p. 121434, Apr. 2023, https://doi.org/10.1016/j.memsci.2023.121434

[32] Y. Chang Kim and T. Min, "Influence of osmotic mediation on permeation of water in reverse osmosis: Experimental and numerical analysis," *Journal of Membrane Science*, vol. 595, p. 117574, Feb. 2020, https://doi.org/10.1016/j.memsci.2019.117574

[33] S. J. Moon, S. M. Lee, J. H. Kim, S. H. Park, H. H. Wang, J. H. Kim, and Y. M. Lee, "A highly robust and water permeable thin film composite membranes for pressure retarded osmosis generating 26 $W \cdot m^{-2}$ at 21 bar," *Desalination*, vol. 483, p. 114409, Jun. 2020, https://doi.org/10.1016/J.DESAL.2020.114409

[34] S. G. Salinas-Rodríguez, Siobhan, J. C. Schippers, and M. D. Kennedy, "Particulate fouling," *IWA Publishing eBooks*, pp. 85–124, May 2021, https://doi.org/10.2166/9781780409863_0085

[35] A. F. Al-Alawy, "Forward and Reverse Osmosis Process for Recovery and Re-use of Water from Polluted Water by Phenol," *Journal of Engineering*, vol. 17, no. 4, pp. 912–928, 2011. https://doi.org/10.31026/j.eng.2011.04.20

[36] L. F. Greenlee, D. F. Lawler, B. D. Freeman, B. Marrot, and P. Moulin, "Reverse osmosis desalination: Water sources, technology, and today's challenges," *Water Research*, vol. 43, no. 9. Elsevier Ltd, pp. 2317–2348, 2009, https://doi.org/10.1016/j.watres.2009.03.010

[37] G. Han and T.-S. Chung, "Robust and High Performance Pressure Retarded Osmosis Hollow Fiber Membranes for Osmotic Power Generation," *AIChE Journal*, vol. 60, no. 3, pp. 1107–1119, 2014, https://doi.org/10.1002/aic.14342

استخدام أنظمة RO–OARO الهجينة كطرق جديدة لعملية تحلية المياه

حسنين عباس حسن [١،*]، أحمد فائق العلوي [١]، مؤيد الشاعلي [٢]

١ قسم الهندسة الكيمياوية، كلية الهندسة، جامعة بغداد، بغداد، العراق
٢ جامعة لوكسمبورغ، لوكسمبورغ

الخلاصة

إن ندرة المياه العذبة ودورها الأساسي في الحفاظ على الحياة على الأرض قد حفزت الباحثين على البحث عن تقنيات جديدة ومنخفضة التكلفة وقابلة للتطوير لتحلية المياه. لهذا، فإن عملية غشاء التناضح العكسي المدعوم تناضحيًا (OARO) تمثل نهجًا مبتكرًا لتحقيق استخلاص معتدل للمياه من المياه عالية الملوحة دون الخضوع لتغيير الطور. يهدف هذا العمل إلى دراسة أداء أنظمة OARO و RO–OARO الهجينة عبر تصميمات وظروف تشغيلية مختلفة على نسب الاسترداد والرفض. تم تقييم الأنظمة الهجينة لمدة ٦٠ دقيقة عند تركيزات تغذية ٣,٩٨–٥,٥٤ غم/لتر، وضغوط مطبقة تتراوح من ٣ إلى ٧ بار، وأنواع مختلفة من الأغشية. أظهرت النتائج أن التدفق للنظام الهجين يزداد بزيادة الضغط وينخفض بزيادة تركيز اللقيم (المغذي). تم الحصول على أعلى قيمة استرداد لنظام RO–OARO عند ضغط RO يبلغ ٧ بار ووحدة OARO عند ٣ بار لتركيز اللقيم قدره ٣,٩٨ غم/لتر. في المقابل، عندما تم تثبيت ضغط التناضح العكسي عند ٥ بار وزاد ضغط وحدة OARO بمقدار ٢ بار، تجاوزت قيمة الاسترداد بحوالي ٦%. علاوة على ذلك، أظهر غشاء FilmTech أعلى نسبة استرداد بلغت ٣١,٧%، بينما أعلى نسبة رفض بلغت ٩٤,٥٥% لغشاء AquaTec. ساهم نظام RO–OARO–OARO في زيادة قيم الاسترداد والرفض بنسبة ١١,٤ و٢,١% على التوالي مقارنة بنظام RO–OARO. كشفت التجارب في هذه الدراسة عن زيادة طفيفة في تركيز المغذي لوحدة التناضح العكسي مما يدل على كفاءة الأنظمة الهجينة مقارنة بأنظمة التناضح العكسي التقليدية.

الكلمات الدالة: هجين، التناضح العكسي، التناضح العكسي المدعوم تناضحيًا، تحلية المياه.